As_2S_8 planar waveguide: refractive index changes following an annealing and irradiation and annealing cycle, and light propagation features*

Zou Liner(邹林儿)[1,†], Wang Gouri(王国日)[1], Shen Yun(沈云)[1], Chen Baoxue(陈抱雪)[2], and Mamoru Iso(矶守)[3]

[1]Department of Physics, Nanchang University, Nanchang 330031, China
[2]School of Optical-Electrical and Computer Engineering, University of Shanghai for Science and Technology, Shanghai 200093, China
[3]Department of Chemical Engineering, Tokyo University of Agriculture and Technology, Tokyo 184-8588, Japan

Abstract: The refractive index of as-evaporated amorphous semiconductor As_2S_8 film upon an annealing and saturation irradiation and annealing cycle is reversible. Upon successive treatment with annealing and non-saturation irradiation and further annealing, the refractive index of the as-evaporated amorphous semiconductor As_2S_8 film reaches a maximum value and then its reversibility occurs upon annealing. The annealing of the amorphous semiconductor As_2S_8 films results in the stabilization of the structure through changes of the S–S bonds in the nearest environment, accompanied by a decrease of film thickness. The As_2S_8 planar waveguide after annealing (130 ℃) and saturation irradiation and annealing (130 ℃) shows a good propagation characteristic with ca. 0.27 dB/cm low propagation loss of the 632.8 nm guided mode.

Key words: amorphous semiconductor chalcogenide; As_2S_8 waveguide; refractive index; light propagation
DOI: 10.1088/1674-4926/32/11/112004 **PACC:** 7280N; 7865M; 4282

1. Introduction

Amorphous semiconductor chalcogenide glasses are potentially useful materials for integrated nonlinear optical components offering low-phonon energies, ultra-fast broadband optical response times and optical transparency in the IR region[1−4]. These unique optical properties make them very interesting for integrated optical devices, all-optical signal processing, optical circuits and, eventually, optical computing[5−8]. Published studies have mostly dealt with stoichiometric As_2S_3 compositions in infrared optical applications. However, because the average covalent bond coordination number of amorphous semiconductor As_2S_8 is lower than that of amorphous semiconductor As_2S_3 and also because of the higher density of chemical bond defects produced by its abnormal electronic configuration, there are a larger number of sublevels in the band gap of amorphous semiconductor As_2S_8[9, 10], especially for amorphous semiconductor As_2S_8 film. More interestingly, a photo-optical effect with an optical stopping function in amorphous As_2S_8 film has been reported in our studies[11], which is not observed in amorphous semiconductor As_2S_3 films. This function is realized through electron transition in sublevels absorbing signal light, however, in amorphous semiconductor As_2S_8, band gap light excites electrons to the sublevels. This optical stopping function will be expected in the development of new waveguide devices with an optical switch function or optical attenuation, so it is necessary to fabricate a low-loss As_2S_8 planar waveguide. Considering that the annealing treatment can improve certain film properties[12, 13], such as adhesion to the substrate, density and physical stability, the films are processed by a cycle of annealing and irradiation, and annealing.

In this paper, the refractive index changes of as-evaporated amorphous semiconductor As_2S_8 films are investigated following an annealing and irradiation and annealing cycle. During the cycle of annealing and saturation irradiation and annealing, the reversibility of the refractive index changes is observed at an annealing temperature of below 160 ℃. After annealing near the glass transition temperature (130 ℃), the refractive index changes are fully reversible. However, with the annealing and non-saturation irradiation and annealing cycle, the refractive index changes continuously increase to the maximum value, and then display reversibility upon further annealing. The light propagation experiment demonstrates the As_2S_8 planar waveguide upon annealing (130 ℃) and saturation irradiation and annealing (130 ℃), and shows a good propagation characteristic with a low loss of 0.27 dB/cm.

2. Experiments

Appropriate atomic proportions of high purity (4N) elemental As and S were sealed under vacuum in cylindrical silica ampoules. The starting materials were then reacted by heating to 800 ℃ and melt homogenized by continuous rocking in a furnace for 48 h. They were then allowed to cool naturally to room temperature in the furnace to form As_2S_8 glass powder. Film samples were fabricated by evaporating the melt-cooled As_2S_8 glass powder from a tantalum boat onto non-refrigerated quartz substrates in a vacuum of 1×10^{-3} Pa with about 10 Å/s, forming a planar waveguide. The film thickness was

* Project supported by the National Natural Science Foundation of China (Nos. 60967003, 61077042) and the Scientific Research Program Foundation of Jiangxi Provincial Education Department, China (No. GJJ11303).
† Corresponding author. Email: zle_jy@yahoo.com.cn
Received 23 April 2011, revised manuscript received 30 May 2011

controlled by adjusting the weight of the powder. The chemical compositions of the films were ascertained by electron microprobe X-ray analyses within an accuracy of ±2 at.%. Annealing was performed in a flowing nitrogen ambient for 1 h and the samples were measured at room temperature. A prism coupling technique using a 1.5 mW 632.8 nm He–Ne laser probe light was employed to measure the refractive index. A UV light with an intensity of 58 mW/cm^2 and a wavelength of 300–436 nm was employed to study the photo-induced changes in the refractive index of the As_2S_8 film. The UV light came from a photolithography source, where the non-uniformity of illumination intensity was less than 3 %. The Raman spectra were measured by using a Fourier transform IR spectrometer with 1064 nm excitation coming from a Nd-YAG laser. The surface morphologies of the film samples were studied by using an FEI Quanta 200F scanning electron microscope (SEM).

3. Results and discussions

3.1. Refractive index changes of the As_2S_8 film upon the annealing and saturation irradiation and annealing cycles

The as-evaporated amorphous semiconductor As_2S_8 film was first annealed and then exposed to UV light for about 70–80 min until its refractive index reached a maximum value. Such a process is called an annealing and saturation irradiation cycle. This cycle was repeated several times. Figure 1 shows the changes in refractive index with UV irradiation for As_2S_8 films during several cycles. Annealing was performed for 1 h in each case at 120,130 or 165 ℃. For repeated annealing at 120 ℃ followed by UV exposure for 80 min in each annealing and saturation irradiation cycle, the refractive index is higher after each annealing step before UV irradiation (i.e., at $t = 0$) and the change in refractive index with irradiation time differs in each cycle. With repeated annealing at 130 ℃, however, the samples before irradiation have the same value of refractive index in each cycle (ca. 2.320), and the refractive index increases with UV irradiation time in a similar manner in each cycle by a further 0.015 after 80 min. After repeated annealing at 165 ℃, the refractive index decreases after each annealing step before UV irradiation (i.e., at $t = 0$) and is lower than the value of the refractive index in the well irradiated sample after repetitious annealing and saturation irradiation cycles. These results indicate that the change in the photorefractive index in the annealed films is reversible by subsequent annealing (note that the whole process consists of the annealing and saturation irradiation and annealing cycle). At an annealing temperature of 130 ℃, the refractive index change is fully reversible. The full reversibility of this phenomenon potentially allows As_2S_8 to be used as a thermally erasable medium and is useful for the experimental fabrication of As_2S_8 strip waveguides.

This reversible phenomenon near T_g (130 ℃) is more evident than that at below T_g (such as 120 ℃). For the annealing temperature near T_g, after each cycle, the refractive index changes are basically the same as with the first cycle; while below T_g, the refractive index change is lower than that of the first cycle, but then has the same trend after the first cycle. Moreover, the average changes of the refractive index Δn after annealing (130 ℃) and saturation irradiation cycles is

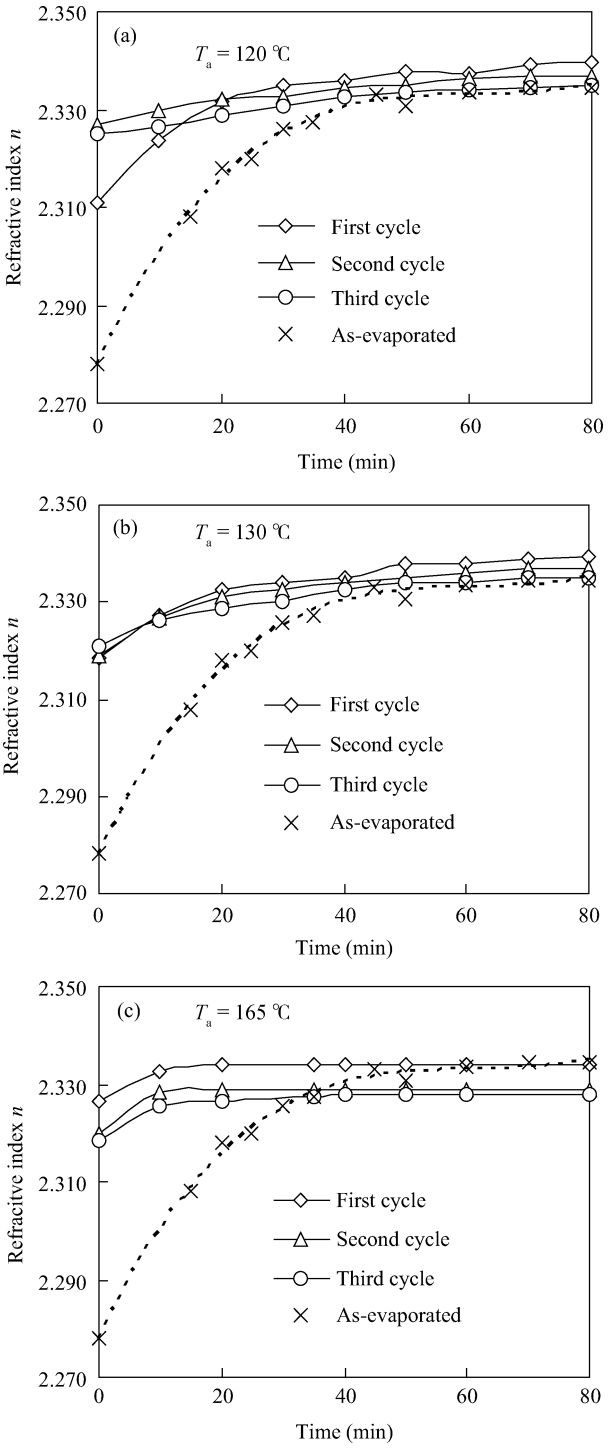

Fig. 1. Refractive index change of As_2S_8 films with repeated annealing and UV saturation irradiation cycles at (a) 120, (b) 130 and (c) 165 ℃. The dashed line denotes the dependence of the refractive index of the as-evaporated film on exposure time under UV light without annealing, compared with the successive annealing and saturation irradiation cycle.

0.018, and is greater than 0.010 after annealing (120 ℃) and saturation irradiation cycles. In general, after the as-evaporated amorphous semiconductor chalcogenide film is annealed near the T_g, the structure of film becomes a stable equilibrium state through the redistribution of chemical bonds. Then, under irradiation, photo-excited carriers are rapidly localized to a range

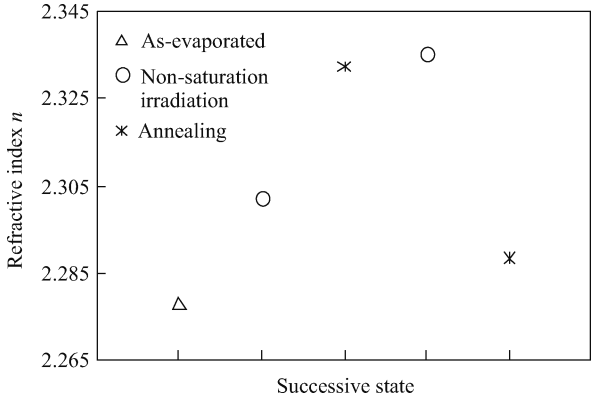

Fig. 2. Refractive index change of amorphous semiconductor As_2S_8 film upon the successive non-saturation irradiation (10 min) and annealing (130 ℃, 1 h) and non-saturation irradiation (10 min) and annealing (130 ℃, 1 h).

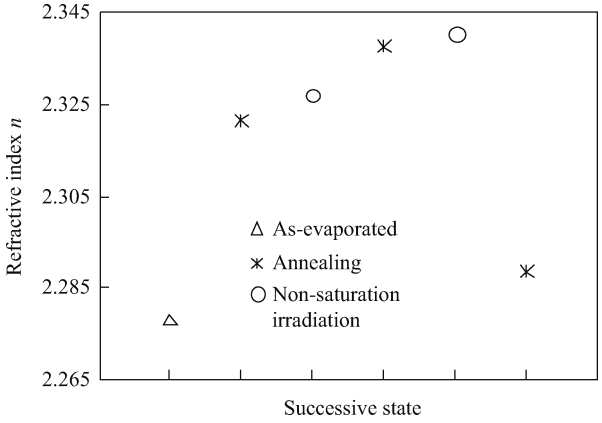

Fig. 3. Refractive index change of amorphous semiconductor As_2S_8 film upon successive annealing (130 ℃, 1 h) and non-saturation irradiation (10 min) and annealing (130 ℃, 1 h) and non-saturation irradiation (10 min) and annealing (130 ℃, 1 h).

of a few angstroms with resulting recombination-induced bond rearrangements, leading to the deformation of the microstructure of the film accompanied by an increase of the refractive index. Upon further annealing, however, thermodynamic activity can accelerate the relaxation of the film and makes the film relax the stable structure by erasing the increase of the refractive index. This reversible phenomenon is also explained from the configuration coordinate of amorphous chalcogenide film[14, 15]. A band gap irradiation for an annealed film induces a transition of defects from a stable state to a quasi-stable state, leading to a change in the local structural order in the amorphous network. With annealing treatment, defects with a quasi-stable state relax thermally to a stable state. Especially under annealing near T_g, most defects are relaxed to a stable state and the film structure is restored to its initial state.

3.2. Refractive index changes of As_2S_8 film upon the annealing and non-saturation irradiation and annealing cycles

The refractive index changes of as-evaporated amorphous semiconductor As_2S_8 films after successive non-saturation irradiation and annealing, and successive annealing and non-saturation are shown in Figs. 2 and 3, respectively. During a period of non-saturation irradiation, the irradiation time is about 10 min less than the saturation irradiation time of about 80 min shown in Fig. 1 and does not lead to the increase of the refractive index to the maximum value. In Fig. 2 (note that the successive state is along the non-saturation irradiation and 130 ℃ annealing and non-saturation irradiation, and then 130 ℃ annealing), the refractive index of the amorphous semiconductor As_2S_8 film increases monotonously from the value of 2.2780 in the as-evaporated film to the maximum value of 2.3350 after the process of non-saturation irradiation and annealing (130 ℃) and non-saturation irradiation, and then upon annealing (130 ℃) reverts back to 2.2884. This change in the refractive index also takes place in the process of the annealing (130 ℃) and non-saturation irradiation and annealing (130 ℃) and non-saturation irradiation, as shown in Fig. 3. In Fig. 3 (note that the successive state is along the 130 ° C annealing and non-saturation irradiation and 130 ℃ annealing and non-saturation irradiation, and then 130 ℃ annealing), the refractive index reverts from the maximum value of 2.3403 to 2.2885 after annealing (130 ℃). From Figs. 2 and 3, during the successive treatment consisting of non-saturation irradiation and annealing, the refractive index of the amorphous semiconductor As_2S_8 film at first reaches the maximum value and, after that, the reversibility of the refractive index is observed upon annealing.

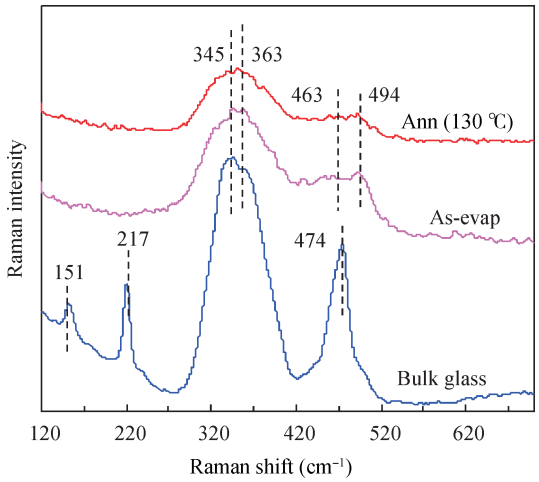

Fig. 4. Raman spectra of the As_2S_8 bulk glass, as-evaporated and annealed (130 ℃) As_2S_8 film.

3.3. Raman and XRD spectra of an amorphous semiconductor As_2S_8 planar waveguide

Annealing is an essential process in the fabrication of optical waveguides, primarily for improving certain film properties, such as adhesion to the substrate, density and physical stability, so a study on annealing induced effects in the films is necessary. Figure 4 shows the Raman spectra of the As_2S_8 bulk glass, the as-evaporated As_2S_8 film and the annealed (130 ℃) As_2S_8 film. The S–S vibration situation is also clear from Fig. 4. In the As_2S_8 bulk glass structure, there are S_8 rings, which give peaks at 151 cm^{-1}, 217 cm^{-1} and 474 cm^{-1}[16, 17]. However, the as-evaporated and annealed

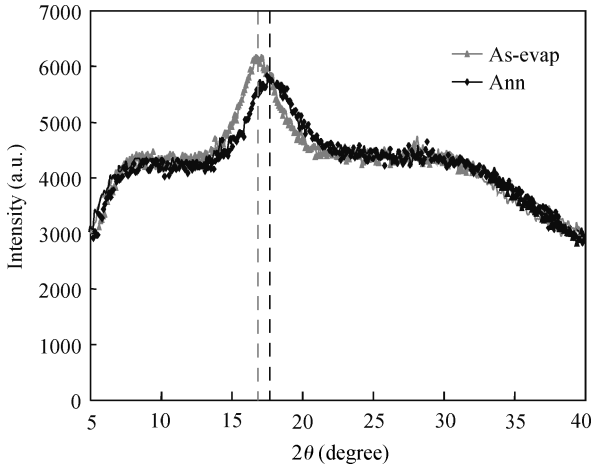

Fig. 5. XRD spectra of the amorphous semiconductor As_2S_8 film sample before (As-evap) and after (Ann) annealing at 130 ℃.

As_2S_8 film structures have no S_8 rings, but have S_n chains instead (the long chains in the broad peak centered at 463 cm^{-1} and the very short chains at 494 cm^{-1} assigned to disulfide bonds, i.e., to very short chains composed of only two S atoms $S_2As–S–S–AsS_2$)[16, 18]. So, the very broad spectral range 420–520 cm^{-1} shows that various types of S–S bonds exist in the As_2S_8 films.

As regards the As–S bonds, it is known that there are no As_4S_4 molecules containing As-As bonds in As–S glasses with As composition lower than the stoichiometric one[19], i.e. $As_{40}S_{60}$. In fact, As_4S_4 realgar molecules with a very strong peak at 185 cm^{-1} are not seen in the Raman spectra of the As_2S_8 films. There are symmetric and antisymmetric modes that give rise to the two peaks at 345 and 363 cm^{-1} for AsS_3 pyramidal units containing As–S bonds[20]. So, the peaks in the 260–420 cm^{-1} range are entirely due to As–S vibrations in pyramids.

Given the above clarification, the structure of amorphous semiconductor As_2S_8 film is better described as a mixture of AsS_3 pyramids and S–S chains. The structural changes are mainly due to changes between S–S bonds in different environments, but not due to changes between homopolar and heteropolar bonds[21, 22]. Then the relative changes of the S–S bonds in the 420–520 cm^{-1} range would become obvious. The relative peaks of molecular fragments such as Sn chains in the Raman spectra of the annealed sample is lower than those in the as-evaporated sample, as shown in Fig. 4. So, the annealing of the As_2S_8 films results in the stabilization of the structure through the changes of the S–S bonds in the nearest environment. As a result, a polymerization of such molecular fragments should be accompanied with a decrease in the thickness of the film. Indeed, a decrease in film thickness upon annealing is observed in Fig. 5.

Figure 5 shows the XRD spectra of the as-evaporated amorphous semiconductor As_2S_8 films obtained using the Cu-Kα line before and after annealing at 130 ℃ for 1 h. Both XRD patterns are broad, indicating that these two films have amorphous structures. The main diffraction peak shifts from 16.80° to 17.50° (2θ) on annealing, corresponding to a reduction in the interlayer spacing from 0.527 to 0.509 nm, which is consistent with the reduction in film thickness. This change found in the XRD patterns suggests a thermal densification of the films. However, upon annealing above 160 ℃, which is near the sulfur polymerization transition temperature of 159 ℃ in S-rich glass[16], it is possible that crystallization effects or sulfur evaporation could be responsible for these effects. These changes under annealing of above 160 ℃ can deteriorate the physical properties of the film sample.

4. Light propagation experiment

To examine the guided light propagation property of an amorphous semiconductor As_2S_8 planar waveguide, a light propagation experiment was investigated. A prism coupling technique was utilized for the guide light propagation experiment in 1-μm-thick As_2S_8 films. The propagation loss of the planar waveguide is estimated through the charge coupled device (CCD) photography[23]. The relative intensities of the scatter light points in the propagation line are recorded by a CCD, transformed into the intensities of the propagation light in the waveguide and then fitted to an exponential decay curve. An attenuated propagation coefficient is calculated by using the exponential decay curve. Guide modes (TE) of wavelength 632.8 nm (He–Ne laser) were generated with a TiO_2 prism coupler. Figures 6(a) and 6(b) show the exponential decay curves with the attenuate coefficient of the light propagation in the as-evaporated amorphous semiconductor As_2S_8 planar waveguide before and after annealing (130 ℃) treatment, and saturation irradiation and annealing (130 ℃), respectively. It is found that the light propagation distance of the as-evaporated amorphous semiconductor As_2S_8 film waveguide, after being processed by annealing (130 ℃) and saturation irradiation and annealing (130 ℃), increases very obviously and its waveguide propagation loss is calculated as ca. 0.27 dB/cm less than that of ca. 1.13 dB/cm in the only as-evaporated amorphous semiconductor As_2S_8 film, which implies that the property of guided light propagation can be improved remarkably by means of this process. This is because the annealing (T_g) and saturation irradiation and annealing (T_g) cycle can relax the structure of the as-evaporated As_2S_8 film waveguide into a stable equilibrium, leading to a decrease of light propagation loss due to an improvement of the surface roughness and density uniformity of the film. Figures 7(a) and 7(b) show the SEM photos of the surface roughness of the as-evaporated amorphous semiconductor film sample before and after the above process treatment, indicating that the surface roughness of the film sample is improved obviously after the treatment and its surface becomes very smooth. Therefore, this process can reduce diffraction loss, leading to a decrease of propagation loss.

After annealing at above more than T_g, such as 165 ℃, however, the light propagation loss increases to two orders of magnitude due to crystallization effects (or phase transformation) at the high annealing temperature[24].

5. Conclusions

In summary, amorphous semiconductor As_2S_8 films prepared by vacuum evaporation were confirmed to undergo changes in refractive index upon annealing and irradiation and annealing cycles. The reversibility of the refractive index is ob-

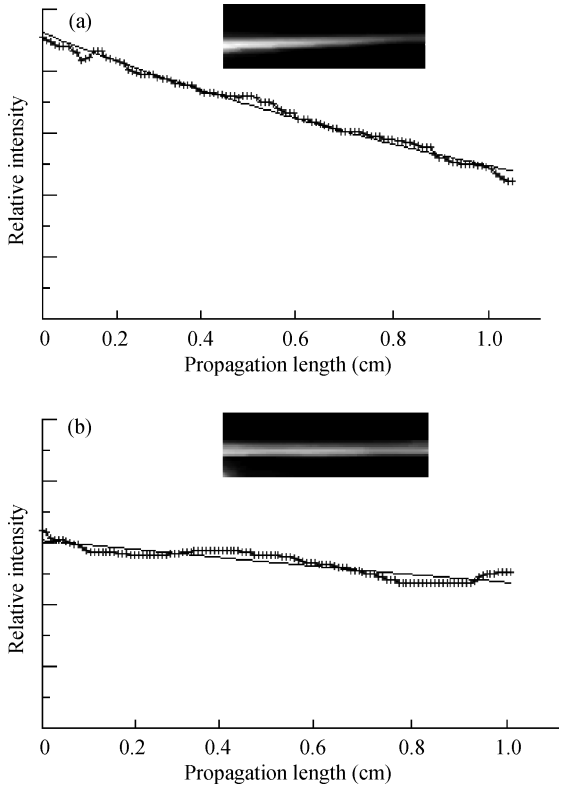

Fig. 6. Relative intensity distribution and its fitting curve of the light propagation line in the as-evaporated amorphous semiconductor As_2S_8 planar waveguide (a) before and (b) after treatment with annealing (130 ℃) and saturation irradiation and annealing (130 ℃). In (a) and (b), the light propagation loss is 1.13 dB/cm and 0.27 dB/cm, respectively. The propagation line images are inset. The short line is the distribution of the relative intensities; the solid line is an exponential attenuated curve fitting.

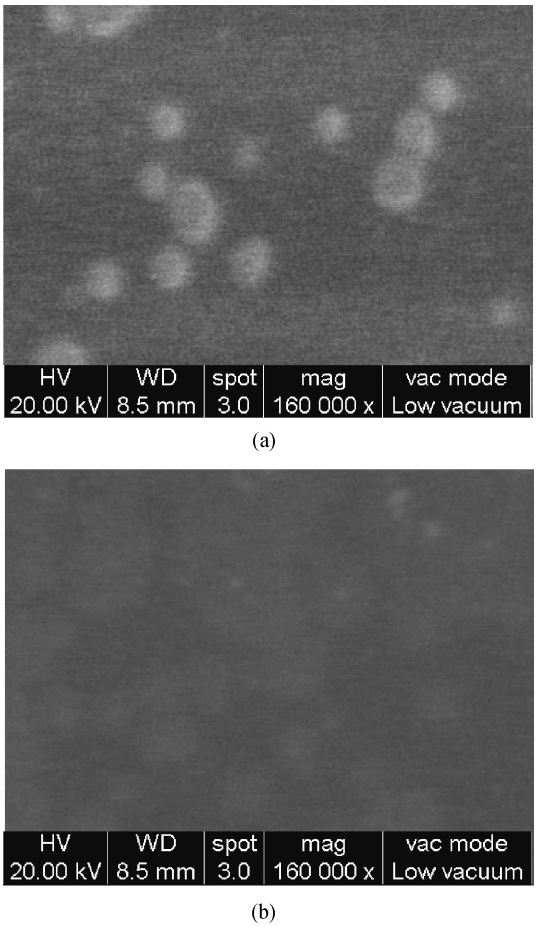

Fig. 7. SEM photos of the surface of the as-evaporated amorphous semiconductor film samples (a) before and (b) after the process of the annealing (130 ℃) and saturation irradiation and annealing (130 ℃).

served on the cycle of the annealing and saturation irradiation and annealing, and especially on annealing near the glass transition temperature (130 ℃), this reversibility is fully reversible, which allows amorphous semiconductor As_2S_8 film to be used as a thermally erasable medium. Upon the cycle of the annealing and non-saturation irradiation and annealing, the refractive index increases continuously to reach the maximum, and then reverts back to the value of about 2.288 upon annealing near the T_g. Annealing near the T_g of the As_2S_8 films results in the stabilization of the structure through these changes between S-S bonds in the nearest environment. The light propagation experiment shows that the as-evaporated amorphous semiconductor As_2S_8 planar waveguide after processing by annealing (130 ℃) and saturation irradiation and annealing (130 ℃) has a good propagation characteristic with a propagation loss as low as ca. 0.27 dB/cm owing to the enhancement of the structural stabilization and the improvement of the surface roughness. The mechanism demonstrated in the present study allows As_2S_8 to be applied in waveguide devices and potentially in a range of other optical applications.

References

[1] Schulte A, Rivero C, Richardson K, et al. Bulk-film structural differences of chalcogenide glasses probed in situ by near-infrared waveguide Raman spectroscopy. Opt Commun, 2001, 198: 125

[2] Van Popta A C, DeCorby R G, Haugen C J, et al. Photoinduced refractive index change in As_2Se_3 by 633 nm irradiation. Opt Express, 2002, 10: 639

[3] Asobe M, Suzuki K, Kanamori T, et al. Nonlinear refractive-index measurement in chalcogenide-glass fibers by self-phase modulation. Appl Phys Lett, 1992, 60: 1153

[4] Asobe M, Kanamori T, Naganuma K, et al. Third-order nonlinear spectroscopy in As_2S_3 chalcogenide glass-fibers. J Appl Phys, 1995, 77: 5518

[5] Viens J F, Meneghini C, Villeneuve A, et al. Fabrication and characterization of integrated optical waveguides in sulfide chalcogenide glasses. J Lightwave Technol, 1999, 17: 1184

[6] Ruan Y, Li W, Jarvis R, et al. Fabrication and characterization of low loss rib chalcogenide waveguides made by dry etching. Opt Express, 2004, 12: 5140

[7] Prasad A, Zha C J, Wang R P, et al. Properties of $Ge_xAs_ySe_{1-x-y}$ glasses for all-optical signal processing. Opt Express, 2008, 16: 2804

[8] Balan V, Vigreux C, Pradel A, et al. Chalcogenide glass-based rib ARROW waveguide. J Non-Cryst Solids, 2003, 326/327: 455

[9] Adler D. Defects in amorphous semiconductors. J Non-Cryst Solids, 1980, 35/36: 819

[10] Borisova Z U. Glassy semiconductors. New York: Plenum Press, 1981

[11] Zou L E, Chen B X, Chen L, et al. Fabrication of an As_2S_8 stripe waveguide with optical stopping effect by exposure to ultraviolet

irradiation. Appl Phys Lett, 2006, 88: 153510
[12] Zou L E, Chen B X, Lin H S, et al. Fabrication and propagation characterization of As_2S_8 chalcogenide channel waveguide made by UV irradiation annealing. Appl Opt, 2009, 48(33): 6442
[13] Zou Liner, Chen Baoxue, Du Liping, et al. Effect of annealing temperature on amorphous semiconductor As_2S_8 film waveguide. Chinese Journal of Semiconductors, 2007, 28: 1307
[14] Liu Q M, Gan F X. Photobleaching in amorphous GeS_2 thin films. Mater Lett, 2002, 53(6): 411
[15] Liu Qiming, Gan Fuxi. Photodarkening in amorphous As_2S_3 thin films. Chin Phys Lett, 2002, 19: 124
[16] Andrikopoulos K S, Kalampounias A G, Yannopoulos S N. Rounding effects on doped sulfur's living polymerization: the case of As and Se. Phys Rev B, 2005,72: 014203
[17] Kalampounias A G, Andrikopoulos K S, Yannopoulos S N. Probing the sulfur polymerization transition *in situ* with Raman spectroscopy. J Chem Phys, 2003, 118: 8460
[18] Kyriazis F, Chrissanthopoulos A, Dracopoulos V, et al. Effect of silver doping on the structure and phase separation of sulfur-rich As–S glasses: Raman and SEM studies. J Non-Cryst Solids, 2009, 355: 2010
[19] Yannopoulos S N. An intramolecular structural model for photo-induced plasticity in a chalcogenide glass. Phys Rev B, 2003, 68: 064206
[20] Kyriazis F, Yannopoulos S N. Colossal photostructural changes in chalcogenide glasses: a thermal photoinduced polymerization in As_xS_{100-x} bulk glasses revealed by near-bandgap Raman scattering. Appl Phys Lett, 2009, 94: 101901
[21] González-Leal J M, Vlcek M, Prieto-Alcon R, et al. Thermal relaxation of the structural and optical properties of amorphous $As_{40}S_{60-x}Se_x$ films. J Non-Cryst Solids, 2003, 326/327: 146
[22] Kolobov A V, Adriaenssens G J. On the mechanism of photo-structural changes in As-based vitreous chalcogenides: microscopic, dynamic and electronic aspects. Philos Mag B, 1994, 69: 21
[23] Jiang Y, Cao Z Q, Chen Y L. CCD camera photographing in detecting the propagation attenuate coefficient of polymer waveguides. J Shanghai Jiaotong University, 1997, 31: 42
[24] Chen P, Holbrook C, Boolchand P, et al. Intermediate phase, network demixing, boson and floppy modes, and compositional trends in glass transition temperatures of binary As_xS_{1-x} system. Phys Rev B, 2008, 78: 224208